Epigenetic upregulation of carotid body angiotensin signaling increases blood pressure.

Fengli Zhu[1], Hayden McSwiggin[1], Jekaterina Zyuzin[1], Jie Liu[1], Wei Yan[1, 2, 5], Virender K. Rehan[1, 3, 5], Nicholas Jendzjowsky[1, 4, 5]

[1]The Lundquist Institute for Biomedical Innovation at Harbor-UCLA, Torrance, CA 90502, USA
[2]Division of Metabolic Diseases and Translational Genomics, Harbor-UCLA Medical Center, Torrance, CA 90502
[3]Division of Neonatology, Harbor-UCLA Medical Center Torrance, CA 90502, USA
[4] Division of Respiratory and Critical Care Medicine and Physiology, Harbor-UCLA Medical Center, Torrance, CA 90502, USA
[5]David Geffen School of Medicine, Los Angeles, CA 90073, USA

*Corresponding Author: Nicholas Jendzjowsky, PhD
Rm 209 Martin Research Building,
The Lundquist Institute for Biomedical Innovation at Harbor-UCLA Medical Center
Division of Respiratory and Critical Care Medicine and Physiology, David Geffen School of Medicine, UCLA
1124 W Carson Street
Torrance, CA
90502-2006
Office:323-457-1663
Email: nicholas.jendzjowsky@lundquist.org

Abstract

Epigenetic changes can be shaped by a wide array of environmental cues as well as maternal health and behaviors. One of the most detrimental behaviors to the developing fetus is nicotine exposure. Perinatal nicotine exposure remains a significant risk factor for cardiovascular health and in particular, hypertension. Increased basal carotid body activity and excitation are significant contributors to hypertension. This study investigated the epigenetic changes to carotid body activity induced by perinatal nicotine exposure resulting in carotid body-mediated hypertension. Using a rodent model of perinatal nicotine exposure, we show that angiotensin II type 1 receptor signaling is upregulated in the carotid bodies of nicotine-exposed offspring. These changes were attributed to an upregulation of genetic promotion as DNA methylation of AT1r and PKC occurred within intron regions, exemplifying an upregulation of genetic transcription for these genes. Nicotine increased angiotensin signaling *in vitro*. Carotid body reactivity to angiotensin was increased in perinatal nicotine-exposed offspring compared to control offspring. Further, carotid body denervation reduced arterial pressure as a result of suppressed efferent sympathetic activity in perinatal nicotine-exposed offspring. Our data demonstrate that perinatal nicotine exposure adversely affects carotid body afferent sensing, which augments efferent sympathetic activity to increase vasoconstrictor signaling and induce hypertension. Targeting angiotensin signaling in the carotid bodies may provide a way to alleviate hypertension acquired by adverse maternal uterine environments in general and perinatal nicotine exposure in particular.

Abstract word count: 228

Key words: Carotid body, sympathetic nervous activity, angiotensin, nicotine, epigenetic, developmental programming

Introduction

Adverse developmental programming is directly related to cardiovascular disease in later life. The epigenetic modifications that occur in response to intra-uterine alterations have lasting effects and are known to alter cardiovascular structure and function in response to several environmental factors and maternal behaviors[1–5]. One of the most detrimental maternal behaviors during the perinatal period, which can deleteriously predispose offspring to cardiovascular diseases, is nicotine exposure, typically in the form of tobacco product use[6].

Perinatal tobacco smoke/nicotine exposure has been shown to augment blood pressure and increase the risk of hypertension in later life[2,6,7]. Arteriolar wall thickening and increased vasoconstrictor signaling are thought to be the primary cause of perinatal smoke/nicotine exposure-induced hypertension[8–10]. Nicotine stimulates the renin-angiotensin-aldosterone system[11] and increases both angiotensin-converting enzyme activity[12,13] as well as angiotensin II type 1 receptor expression and activity[12–14] within the aorta[15–17] and mesenteric arterioles[16,18]. Such arteriolar reactivity would likely implement a hypertensive state.

Aberrant sympathetic nerve activity is significantly tied to cardiovascular disease and a prime mediator of hypertension in a multitude of cardiometabolic diseases[19,20]. Carotid bodies are polymodal sensors that regulate sympathetic nervous activity to control vasoconstriction to regulate tissue oxygen/nutrient delivery[21,22]. Indeed, hypertension appears to be critically dependent on tonic input from carotid bodies to augment sympathetic tone[19,20]. Carotid bodies appear to be sensitized in nicotine-exposed offspring as their tonic activity is not suppressed with hyperoxia, which typically quiesces carotid body excitation[23,24]. Given their primary role in stimulating arteriolar vasoconstriction[19,20] and their susceptibility to nicotine exposure[23,24], the carotid bodies are likely susceptible to epigenetic modulation because of developmental programming[25–27], which would lead to an elevation of tonic activity. Therefore, we investigated the possibility that the carotid bodies and epigenetic responses therein are prime culprits for hypertension in perinatal nicotine-exposed offspring.

Guided by an unbiased transcriptomic analysis, we identified that angiotensin and associated signaling transcripts are altered in the carotid bodies of perinatal nicotine-exposed offspring. The unbiased transcriptomic screen was confirmed with qPCR. Angiotensin and Angiotensin II type 1 receptor signaling in the carotid bodies are critically important in response to hypoxia[28] and nicotine is known to upregulate angiotensin signaling[11]. Further identification of DNA-protein interactions in the carotid bodies demonstrated that a significant proportion of DNA methylation occurs in the CHG intron sites of Angiotensin and associated genes. *In vitro*, analysis of carotid body-like PC12 cells further showed that nicotine augments PC12-mediated angiotensin signaling pathways, which are likely dependent on terminal TRPV1 phosphorylation. Further, angiotensin delivery to the carotid bodies augments blood pressure reactivity which is suppressed with acute carotid body denervation. Finally, continuous blood pressure and concurrent sympathetic nervous activity recordings demonstrate that carotid body denervation reduces blood pressure in perinatal nicotine-exposed offspring. These data collectively indicate that the carotid bodies undergo epigenetic modifications in response to maternal programming, which have deleterious consequences on cardiovascular function in later life.

Methods

Animal models, care and ethical standards

First time pregnant Sprague-Dawley (SD) rat dams were purchased from Charles River (Hollister, CA) at gestational day 3. SD mothers were subject to subcutaneous nicotine injections (2mg/kg, Millipore Sigma, PHR2532) from gestational day 7 to post-natal day (PND) 21[29–31]. Control mothers received PBS (vehicle). Experiments on pups took place from PND56-80. Animals were housed with controlled temperature (21 ± 2 °C), humidity (55 ± 10%) and 12 h light-dark cycle. Pups were weaned on PND21 and housed in pairs. Animals had unlimited access to food and water (*ad libidum*). All experimental procedures were approved by The Lundquist Institute for Biomedical Innovation at Harbor UCLA Medical Center IACUC board, protocol # 31659.

Assignment of control or nicotine to mothers was block randomized. Unbiased transcriptomic and genomic sequencing was based on previous data acquired by neuronal sequencing results. *In vitro* and *in vivo* power calculations were based on an estimated effect size of 50% difference with assumed unified standard deviation across groups.

Carotid body next generation sequencing

Next generation RNA sequencing- On PND 56, animals were sedated (5% isoflurane, balance O2), exsanguinated and carotid bodies gross dissected and placed in a sylgard coated dissecting dish filled with Ham's F12 media. Carotid bodies were then freed from the carotid arch under a dissecting microscope. Five carotid body pairs (n=10 carotid bodies from 5 rats) from each group and sex (n=5 rats per group, per sex) were lysed and RNA was isolated using the easy-spin Total RNA extraction kit (Boca scientific, Cat. # 17221). RNA integrity was tested with Nanodrop spectrophotometer (Thermofisher Cat. # ND2000USCAN) and deemed to be of appropriate quality of A260/280 was between 1.99 and 2.10. RNA sequencing was then conducted by an unbiased commercial vendor (Novogene corporation, Sacramento CA), where further integrity (RIN >7) and downstream processing and analysis took place.

DNA-bisulfite sequencing- Carotid bodies were dissected as above. Five carotid body pairs (n=10 carotid bodies from 5 rats) from each group and sex (n=5 rats per group, per sex) were lysed and DNA was isolated using the QIAamp UCP DNA Micro Kit (Qiagen, Cat. # 56204). DNA integrity was deemed sufficient with A260/280 1.75-1.85. Bisulfite conversion and downstream whole-genome DNA-bisulfite sequencing were conducted by (Novogene Corporation, Sacramento, CA).

qPCR- an additional group of n=3 samples (n=5 rats per sample) from each group was harvested as above. RNA was converted to cDNA using the Tetro cDNA synthesis kit (Meridian life sciences, Cat. # Bio65043). qPCR was conducted with Taqman specific probes for AGTR1 (Thermofisher Rn02758772_s1) and TRPV1 (Thermofisher Rn00583117_m1) in reference to HPRT (Thermofisher Rn01527840_m1) using Taqman fast advanced master mix enzyme (Thermofisher Cat. # 4444557) and the QuantStudio 3 thermocycler (Thermofisher Cat. #A28567) using manufacturers instruction. Delta CT was calculated in reference to HPRT and comparisons between group made using unpaired two-sided t-test.

Immunohistochemistry

Carotid bodies were gross dissected as above. Then they were cleaned from connective tissue but left attached to the surrounding carotid artery bifurcation as previously[32]. Tissues were fixed in 4% paraformaldehyde for 1-2hours at 4°C, then cryopreserved in 30% sucrose overnight at 4°C, dried embedded in OCT and cut at 14µm sections on a cryostat. Sections were then

washed (PBS), permeabilized (Triton x 20%) blocked with 10% goat serum (Abcam, Cat. # ab7481) and incubated with antibodies for tyrosine hydroxylase (Millipore Sigma ZMS1033, clone 20/40/15), AGT1R (Millipore Sigma AB15552, polyclonal) and TRPV1 (Alomone Labs, polyconal) for 24hours at 4°C and subsequently stained with appropriate secondaries (Jackson Laboratories Goat-anti rabbit Cy3 111-165-003, Cy5 111-005-003 and Goat-anti mouse 488 115-545-003) for 90 minutes and then counterstained with DAPI (Millipore Sigma MBD0015) and coverslipped with prolong diamond antifade mounting media (Thermofisher #P36970). Slides were imaged using the Leica Thunder imaging acquisition system.

PC12 culture

PC12 cells were cultured in RPMI 1640 (Gibco # 11875093) supplemented with 10% Horse Serum (Gibco Cat. #26050-088) and 5% FBS (Gibco Cat. #F2442), 0.4µg/ml dexamethasone (Millipore Sigma Cat. # D4902) and 1% penicillin/streptomycin (Millipore Sigma Cat. # P0781). Cells were seeded at $3x10^5$ cells in 1ml of media per well (24 well plate, qPCR) or 2500 cells in 150µl of media per well (96 well plate calcium imaging- see below).

qPCR- cells were separated into media (control) or nicotine ((Sigma Cat. # 6019-06-3, 50µg/ml) for 360min then lysed and RNA was isolated using the easy-spin Total RNA extraction kit (Boca scientific, Cat. # 17221). RNA integrity was tested with Nanodrop spectrophotometer (Thermofisher Cat. # ND2000USCAN) and deemed to be of appropriate quality of A260/280 was between 1.99 and 2.10. cDNA was converted using the Tetro cDNA synthesis kit (Meridian Life Sciences Cat. # NC1352749). qPCR was conducted with Taqman specific probes for AGTR1 (Thermofisher Rn02758772_s1) and TRPV1 (Thermofisher Rn00583117_m1) with TH (Thermofisher Rn00562500_m1) and EPAS1 (Rn00576515_m1) as tissue control in reference HPRT (Thermofisher Rn01527840_m1) using Taqman fast advanced master mix enzyme (Thermofisher Cat. # 4444557) and the QuantStudio 3 thermocycler (Thermofisher Cat. #A28567) using manufacturers instruction. N=3 wells were analyzed for each condition for each probe and five separate experiments were run. Delta CT in reference to HPRT were calculated and the average of each experiment used to compare groups. Unpaired two-sided t-test compared conditions.

Calcium imaging- cells were separated into media (control), stimulated with nicotine (Sigma Cat. # 6019-06-3, 50µg/ml), nicotine + angiotensin II (Tocris Cat. # 1158, 5µM), nicotine + angiotensin II + losartan (Tocris Cat. # 3798, 3µM), nicotine + angiotensin II + AMG9810 (TRPV1 antagonist Tocris Cat. # 2316, 10µM) or nicotine + angiotensin II + losartan + AMG9810, for 1 hour and then incubated with Calcium Orange AM methyl ester (Invitrogen Cat. # C3015) + 0.01% Pluronic acid (Invitrogen Cat. #F-127) for 20 minutes, washed in media and then imaged in the Incucyte imaging system (Sartorius) using the Neural imaging parameters (Ex: 549λm/ Em: 576λm, 60s) for 1 hour. The frequency of methyl ester excitation bursts was averaged for each well to express a single value. Data were analyzed with One-way ANOVA using the corrected method of Benjamini and Yekutieli post-hoc test.

In vivo carotid body reactivity

Rats from control or nicotine groups (as above) were tested on PND56-58. Rats were anesthetized with 5% isoflurane (balance room air) using the Kent Scientific Somnosuite anesthesia system. The femoral artery and vein were cannulated, and the arterial line was instrumented to a pressure transducer to measure continuous arterial pressure (AD instruments MLT0670) using the PowerLab data acquisition console (AD instruments PL3516/P). The vein

was then connected to a syringe pump (Fisherscientific Cat. # 14831200) to induce a 15mg/kg/min infusion of alfaxan (Victor Medical Cat. # 1629020) (REF). Then the jugular vein was cannulated to deliver bolus injections of Angiotensin II (Tocris Cat. # 1158 1mg/kg) and NaCN (Fisherscientific Cat. # AA1213722, 200µg/kg). These injections were repeated following bilateral carotid body denervation. Mean arterial pressure was averaged at the 60s preceding each bolus injection and a 60s average during the peak reactive response to each bolus injection. Data were analyzed by Two-way ANOVA (Group x Carotid body intact vs. denervated) for Angiotensin II or NaCN injection. Holm-Sidak post-hoc test determined group differences.

Serum angiotensin concentration

Blood was collected after induction of IV anesthetic but, before any drug infusion from the above experiment from the femoral vein. Blood was left to coagulate for 20minutes on ice then spun at 4,000rpm for 10 minutes at 4°C. Serum was drawn, aliquoted, snap frozen and stored at -80°C until analysis. Angiotensin ELISA (Raybiotech #EIAR-ANGII-1) was used per manufacturer's instructions. Groups (Control pups vs. perinatal nicotine exposed pups) were analyzed with two-sided unpaired t-test.

Arterial pressure assessment between groups

Rats from control or perinatal nicotine-exposed mothers were handled daily following weaning at PND21 and habituated to the tail plethysmography system (IITC Lifesciences). Three-minute averages of tail cuff-measured blood pressure was averaged to attain a single value for each animal. Data were compared using an unpaired two-sided t-test.

Carotid body-mediated changes in arterial pressure

Perinatal nicotine-exposed rats were prepared for telemetric implant between PND56-60. Rats were anesthetized with 5% isoflurane (balance O2) as induction and maintained on a surgical plane with 2-3% isoflurane. The surgical area was isolated, shaved, and treated with 3x betadyne and 3x 70% alcohol. A midline incision was made, and the descending aorta below the renal arteries and renal nerves were isolated. The Kaha telemetry dual sna/pressure (TRM56SP, AD Instruments) were instrumented around the renal nerves using KwikGard dental impression material to isolate electrodes (SNA) and into the aorta as per manufacturer's instructions to measure continuous pressure measurement. The surgical area was sewn in layers, and the skin was secured with surgical staples. Rats were given buprenorphine (0.03mg/kg SQ) 2x daily for three days and allowed to recover for a total of 5 days before commencing recording. Pressure and SNA were recorded for 1 week; then rats were anesthetized as above; the neck area was isolated, shaved, and treated with 3x betadine and 3x 70% alcohol. A midline incision was made on the neck, and the carotid bodies were identified behind the occipital arteries. The carotid sinus nerve was severed bilaterally, the skin sewn with subcuticular sutures. Buprenorphine was delivered as above, and recording commenced for another week following recovery. Pressure waveforms delineated heart rate, systolic, diastolic, and mean arterial pressures. RSNA were filtered, rectified, and integrated using the Lab Chart 8. Data were binned into daily averages and analyzed pre-post with a two-sided paired t-test.

Statistics

Specific statistical tests are described for each experiment above. Data were averaged and analyzed for each experiment as above. Data were analyzed using Graphpad v10.

Results

Epigenetic changes in the carotid body in response to perinatal nicotine exposure

To investigate possible genetic changes expounded by adverse maternal behaviors, we implemented a standardized model of perinatal-nicotine exposure[29–31]. Given that the carotid bodies are prime drivers of hypertension in self-actualized cardiometabolic disease states[22,33], we conducted an unbiased transcriptomic screen of carotid bodies harvested from perinatal nicotine-exposed pups on PND56, 5 weeks after weaning and the final dose of nicotine delivered to the mother. We pooled together carotid bodies from 5 pups in each group of nicotine-exposed and saline control pups (Fig 1a). Samples were analyzed by sex, but no sex difference was found. A total of 922 genes were differentially expressed between conditions, with 685 up-regulated, 237 down-regulated, and 19196 unchanged transcripts (Fig 1b, c). Of these genes, gene-ontology analysis revealed a vast number of highly significant GO pathways however, GO:0004930 was highly significant (1.539 normalized enrichment score; Fig 1d) which included Agt1ra and Agt1ra was significantly upregulated in nicotine-exposed offspring compared to control (0.69 Log2 change, p_{adj}=0.04).

Given that our goal was to elucidate possible epigenetic differences responsible for mediating a neurogenic form of hypertension we probed further and conducted whole genome DNA methylation analysis of the carotid bodies from perinatal nicotine exposed and control pups on PND 56 (Fig 2). Samples were analyzed by sex, but no sex difference was found. Mapping the whole genome of the carotid bodies between groups revealed that the predominant changes to DNA methylation occurred in the promoter (suppression) and intron/exon regions (enhancement Fig 2b,c). Methylation was distributed throughout the genome where a differential set of Genes were altered predominantly on the cytosine-guanine (CG) and cytosine-arginine/threonine/guanine-guanine (CHG) regions (Fig2c-g). GO analyses of whole genes (Fig 2d) and promoter regions (Fig 2f) revealed similar GO terms as with transcriptomic changes. Further, KEGG and analyses of whole genes (Fig 2e) and promoter regions (Fig 2g) were also congruent with pathways associated with neuroactive ligands and GPCRs. Importantly, a significant difference in methylation Agtr1b between groups was demonstrated on CG 7 with a difference of 0.021829. Similarly, protein kinase activity (GO) and, in particular, PRKCE were hypermethylated in exon regions. Given that these methylation changes occurred in regions associated with the upregulation of angiotensin GPCR signaling, we wanted to further investigate the functional outcomes of this pathway. The combined transcriptomic changes and DNA methylation of the whole genome points to an upregulation of angiotensin signaling within the carotid bodies of perinatal nicotine exposed offspring. RNA sequencing and DNA bisulfite sequencing data have been deposited and can be found in the NIH SRA (Bioproject ID: PRJNA1106547).

Validation of transcriptomic and whole genome bisulfite sequencing

To validate these findings, we conducted immunohistochemistry and qPCR with taqman probes to identify possible upregulation of potential signaling pathways in the carotid bodies between perinatal nicotine exposed and control pups. We show that in relation to HPRT, Agt1r was significantly upregulated in perinatal nicotine-exposed offspring compared to control. As, Angiotensin signaling in carotid body microdomains has been previously shown to hinge on post-synaptic expression and regulation of TRPV1 phosphorylation[28], we observed an increase in TRPV1 transcripts from the whole carotid body, although this did not reach statistical

significance (Fig 3). Proteins for Agt1r, TRPV1, and tyrosine hydroxylase (a standard marker of carotid body glomus cells) were all present in sections of carotid bodies harvested from perinatal nicotine-exposed offspring where Agt1r is upregulated on glomus cells and TRPV1 appear to oppose glomus cells on the post-synaptic terminals[28] (Fig 3).

Nicotine upregulates Agtr1 activity

To show that nicotine itself is responsible for Agtr1 upregulation, we used a cell culture model. PC12 cells have been routinely used as a surrogate carotid body glomus cell system[34–36]. Six hours of nicotine exposure significantly upregulated Agt1r (Fig 4a). Differences in Agtr2 and TRPV1 were not demonstrated (Fig 4b&c). Differences between regulatory genes of Hif2α (EPAS- Fig4d) and tyrosine hydroxylase (TH- Fig 4e) were not demonstrated between conditions in relation to the housekeeping gene hypoxyribosyltransferase (HPRT).

Using calcium imaging, we investigated how nicotine would augment glomus cell excitation. We show that with 1 hour of exposure to nicotine, PC12 cells increased their level of calcium spike frequency. Importantly, the addition of angiotensin did not further increase PC12 cell excitation compared to the addition of nicotine and the nicotine + Angiotensin condition showed a significantly higher level of calcium spike activity compared to control media. Further, losartan reduced calcium activity in PC12 cells when delivered to nicotine + angiotensin-stimulated cells concurrently. The reduction in calcium flux was also reduced with AMG9810, a known TRPV1 antagonist, and in combination with TRPV1 and Losartan (Fig 4f). In conclusion, nicotine has a stimulatory effect on PC12 and, quite likely, carotid body glomus cells to increase the expression and excitation of the angiotensin signaling pathway via Agt1r and TRPV1.

Angiotensin acutely increases arterial pressure

To assess acute carotid body reactivity to angiotensin, pups from perinatal nicotine-exposed or control mothers were anesthetized and given a bolus angiotensin injection into the jugular vein before and after acute carotid body denervation (Fig 5a, b). In response to jugular vein injected angiotensin (circulates through the pulmonary circulation, then encounters the carotid bodies), arterial pressure was significantly elevated in nicotine-exposed offspring compared to controls (Fig 5c). In response to sodium cyanide, which blocks mitochondrial complex III and has been routinely used as a carotid body stimulant, there was no significant difference between groups (Fig 5d). Following carotid body denervation, arterial pressure was suppressed and did not respond to angiotensin or sodium cyanide (Fig 5c, d). Importantly, serum harvested from these rats prior to any drug delivery demonstrated that circulating levels of angiotensin were not altered between groups (Fig 5e) similar to previous results[18].

These data demonstrate a significant increase in carotid body excitability in response to angiotensin *in vivo* and suggest a hyperactive angiotensin signaling pathway within the carotid bodies of perinatal nicotine-exposed offspring.

Carotid bodies are responsible for elevated blood pressure in perinatal nicotine-exposed offspring

We evaluated arterial pressure between quiescent conscious control and nicotine exposed offspring using tail cuff plethysmography on PND56. Indeed, arterial pressure was higher in nicotine-exposed offspring (Fig 6a). To definitively demonstrate that the carotid bodies were primarily involved in perinatal nicotine-exposed hypertension, we implanted indwelling telemetry

to measure real-time arterial pressure from the aorta and efferent sympathetic activity directed to the renal nerve between PND56-60 (Fig 6b). We show that within the same animal, carotid body denervation drastically reduces arterial pressure and RSNA (Fig 6b). These data demonstrate that carotid body excitation contributes to the hypertensive state in perinatal nicotine-exposed offspring.

Discussion

Epigenetic changes in response to adverse maternal programming lead to cardiovascular sequelae in later life. Hypertension has been a consistent outcome associated with many adverse intra-uterine insults ranging from undernutrition[37,38], overnutrition[38,39], hypoxia[40,41], and stress[42]. The risk of hypertension is thought to be significantly increased in perinatal nicotine-exposed offspring. The current data demonstrate that epigenetic changes in angiotensin signaling in the carotid bodies mediate hypertension in perinatal nicotine-exposed offspring.

We show, for the first time, that epigenetic modifications in response to adverse maternal programming in the form of nicotine exposure increase angiotensin, angiotensin II type 1R transcripts, angiotensin II type 1R intron, PKC epsilon exon methylation demonstrating an increase in angiotensin signaling in the carotid bodies. These epigenetic changes *in vivo* are confirmed *in vitro* as we show that nicotine directly increases angiotensin signaling in PC12, glomus-like cells, in culture. Blood pressure reactivity to angiotensin is increased, in line with previous investigations, through a neurogenic mechanism involving carotid body-mediated excitation of efferent sympathetic activity. Finally, carotid body denervation reduced blood pressure in perinatal nicotine-exposed rats alongside efferent sympathetic activity.

Clinical data demonstrate that hypertension is likely in offspring that experienced intra-uterine smoke exposure[2,7]; however, the age, sex, and potential for confounding lifestyle factors make it difficult to tease out this association. Pre-clinical data using rodent models show that vascular reactivity to angiotensin via angiotensin II type 1 receptor gene expression, protein expression, and signaling increases in aortae and mesenteric arterioles following prenatal and perinatal nicotine exposure[14,15,18]. Accordingly, increased angiotensin II type 1 R activity, RNA, and DNA methylation[43,44] have been a consistent finding in response to perinatal nicotine-exposed offspring in vascular tissues. Our data show that additional sensory neural systems which are significantly tied to hypertension are also augmented and induce hypertension in perinatal nicotine exposed mice.

To date, scant data are available regarding the effects of nicotine exposure or perinatal nicotine exposure on carotid body activity and resulting autonomic reflex disturbances[23,45]. Carotid bodies are tasked with a multitude of homeostatic control mechanisms that regulate nutrient and oxygen delivery to tissues[21]. Their role in blood pressure regulation is highlighted by genetic[22] and epigenetic[27] modifications demonstrating the ability to increase basal activity and result in augmented blood pressure. Specifically, the spontaneously hypertensive rat (SHR) has augmented carotid body basal activity, which translates to alterations in breathing, blood pressure regulation, and glucose homeostasis[22]. Importantly, these carotid body changes appear to hinge on a significant difference in transcriptomic profile compared to their normotensive genetic counterpart, the Wistar-Kyoto (WKY) rat[22]. Further, and particularly salient to the current argument, carotid body denervation in SHR reduced arterial pressure, whereas carotid body denervation in WKY, had no effect[19]. Importantly, evidence demonstrates that

carotid body basal excitation can change via epigenetic modifications which suppress redox disinhibition[27] to alter basal regulatory mechanisms such as breathing regulation.

A consistent finding is that intrauterine conditions with low oxygen[23] or hyperleptinemia[46] lead to augmented carotid body basal activity. Therefore, it is possible that deficiencies in the intrauterine environment augment arterial pressure in offspring due to the carotid body-regulated mechanism. Our data are the first to demonstrate that adverse maternal programming leads to carotid body epigenetic changes in angiotensin signaling and, importantly, the first to demonstrate that these epigenetic changes occur as a result of genetic upregulation via DNA methylation, which results in carotid body excitation. This carotid body excitation appears to be due to increased angiotensin signaling within the carotid bodies due to increases in carotid body micro signaling domains. Our *in vitro* experiments with PC12 cells demonstrate the epigenetic changes in carotid body angiotensin signaling are as a direct result of nicotine exposure. Further, the reactivity of PC12 cells was regulated by nicotine and a likely intracellular augmentation of angiotensin signaling. In addition to an augmentation of At1r gene expression and gene promotion, PKCs were also methylated on intron regions. PKCs, and in particular PKC subtypes theta and epsilon are known to phosphorylate GPCRs and TRPV1[28,47]. For example, repeated hypoxic bouts increase basal activity via an Angiotensin-TRPV1 mediated mechanism[28]. Given that losartan and TRPV1 blockade suppressed calcium signaling in PC12 cells, with no further reduction in calcium excitation with dual inhibition, we suggest that a similar mechanism is responsible for the augmentation of basal carotid body excitation. These data then fit with the increased carotid body reactivity to angiotensin in an anesthetized preparation and the consistent reduction in arterial pressure with carotid body denervation in conscious perinatal nicotine-exposed offspring.

Perspectives

Carotid body denervation has shown clinical utility, as human clinical trials have shown that unilateral carotid body denervation results in a small but clinically meaningful reduction in human blood pressure[48,49]. We do not recommend such invasive procedures for future therapies. Various tissues express AT1r, and therapeutic delivery to carotid bodies, specifically, has proven difficult. New-generation genetic targeting of tissues has shown promise for AAV tissue specificity[50]. Therefore, we suggest that a targeted suppression or reversal of angiotensin signaling in the carotid bodies of perinatal nicotine exposed offspring would help alleviate increased blood pressure and cardiac afterload and limit unwanted side effects.

Conclusion

Hypertension resulting from perinatal nicotine exposure is due to epigenetic modifications within the carotid bodies. The increased At1r-TRPV1 signaling increases efferent sympathetic activity to augment arterial pressure. Future investigations should target neurogenic signaling mechanisms to alleviate hypertension because of adverse epigenetic programming.

Acknowledgements

This project was supported by T32IP4707 of the Regents of the University of California Tobacco-Related Diseases Research Program (TRDRP). NJ is supported by NIH grant R21AI159221, R56AI175328, UCLA CTSI UL1TR001881-01 and, T32KT408 of the Regents of

the University of California TRDRP. WY is supported by NIH grant P50HD098593 and R01HD099924. VR is supported by NIH grant R01HL151769 and 29IR00737, T32IP5044, T32IR5048, and T32IR5365) of the Regents of the University of California TRDRP. The content is solely the responsibility of the authors and does not necessarily represent the official views of the National Institutes of Health or the UCOP TRDRP. Figures, 1, 2, 5 and 6 were completed with Biorender.

Author contributions

F.Z. & J.K. contributed to experimental design, conducted experiments and analyzed data. H.M and J.L. contributed to experimental execution and data analysis. W.Y. and V.R. assisted with experimental design and analysis. N.J. designed the study, conducted experiments, analyzed data, prepared the manuscript and figures. All authors agree on the manuscript.

Conflict of interest statement

All authors do not declare competing interests.

Figure legends

Figure 1. Perinatal nicotine exposure alters RNA transcripts associated with angiotensin signaling in the carotid body. a) Transcriptomic study design. Nicotine or saline was delivered to the mother on E6 to PND 21. Bilateral carotid body (CB) samples were micro-dissected from perinatal nicotine or saline (control) exposed rats on PND 56. (n=5 rats per group- tissues were pooled to yield sufficient RNA for analysis) One male and one female group per condition. **b)** PCA plot showing distinct separation between nicotine and control groups. PCA1 was group and PCA2 was sex. **c)** Heatmap showing overall differences in RNA distribution. **d)** Gene ontology GSEA plot for G-protein-coupled receptor activity (0004930) where Agt1ra was significantly increased in nicotine-exposed offspring compared to controls.

Figure 2. Perinatal nicotine exposure alters DNA methylation in the carotid body. a) DNA-methylation study design. Nicotine or saline was delivered to the mother on E6 to PND 21. Bilateral carotid body (CB) samples were micro-dissected from perinatal nicotine or saline (control) exposed rats on PND 56. (n=5 rats per group- tissues were pooled to yield sufficient DNA for analysis). One male and one female group per condition. **b)** Circos plot showing differences in C-G methylation sites between perinatal-nicotine exposed and control carotid bodies. **c)** Heatmap displaying C-G and CHG methylation differences in carotid bodies between nicotine and saline-exposed rats. Mapping of methylation changes is confined to the CG and CHG regions as per the heat maps. **d)** Enriched Go terms for C-G methylated DNA between nicotine-exposed and control pups. **e)** Dot plot showing the gene number and enrichment factor of GO pathways between nicotine-exposed and control pups. **f)** KEGG pathway terms for C-G methylated DNA between nicotine-exposed and control pups. **g)** Dot plot showing the gene number and enrichment factor of KEGG pathways between nicotine-exposed and control pups.

Figure 3. Angiotensin II Type 1 receptor is colocalized with TRPV1 at nerve terminal in tyrosine hydroxylase expressing glomus cells. We show that AGT1R is colocalized to glomus cells (express tyrosine hydroxylase, TH) and are adjacent to TRPV1 which are expressed by petrosal ganglion nerve terminals (Carotid bodies synapse onto petrosal ganglia). Scale bar=20µm . qPCR of carotid bodies (n=3 per sample, n=3 samples per group) shows that

AGT1R is upregulated with perinatal nicotine exposure compared to saline control exposed rats. AGT1R- t_4=2.792; TRPV1-t_4=1.735.

Figure 4. Nicotine increases Angiotensin signaling in cultured PC12 cells. a-e) PC12 cells (rat adrenal pheochromocytoma cells resemble carotid body glomus cells) were cultured for 6 hours with and without 50µg/ml nicotine (similar concentration to a single dose of nicotine used *in vivo*), **a)** Agt1R was increased by nicotine (T_8=3.253), **b)** Agtr2 (T_8=0.1899), **c)** TRPV1 (T_8=0.1034)and, regulatory genes of **d)** EPAS (Hif2α; T_8=0.2461) and **e)** Tyrosine hydroxylase (TH- common PC12 and glomus cell marker, T_8=0.1704) were unchanged. Data presented as a relative change of gene expression. **f)** PC12 cells were cultured for 1 hour with media (control) nicotine (Nic, 50µg/ml), Nic + Angiotensin (Ang-50ng/ml), Nic+Ang+Losartan (AII1R blockade 3µM), Nic+Ang+AMG9810 (TRPV1 blockade 10µM), Nic+Ang+Losartan+TRPV1x and imaged for calcium flux using Incucyte calcium imaging with Calcium Orange (forms Calcium esther complex- non-ratiometric imaging). $F_{5,44}$=4.485.

Figure 5. Carotid body reactivity to angiotensin is increased in perinatal nicotine-exposed pups compared to control with unaltered serum angiotensin. a) Diagram of *in vivo* experimental preparation- serum was isolated before injection of angiotensin or NaCN. **b)** A representative trace of arterial pressure of vehicle and perinatal nicotine-exposed pups on P56 in response to a bolus jugular vein IV injection of angiotensin. **c)** The increase in arterial pressure in response to angiotensin in vehicle (grey) and perinatal-nicotine exposed pups (red) before and following carotid body denervation $F_{1, 11}$=5.207). **d)** The increase in arterial pressure in response to NaCN in vehicle (grey) and perinatal-nicotine exposed pups (red) before and following carotid body denervation $F_{1, 11}$=0.1595). **e)** Serum was harvested before administration of bolus injections (T_{14}=0.8077).

Figure 6. Perinatal nicotine-exposed rats have increased mean arterial pressure mediated by carotid body augmentation of sympathetic activity. a) Mean arterial pressure, as assessed by tail-cuff plethysmography, was augmented in nicotine-exposed offspring compared to controls (T_{20}=7.964). N=11 per group, 2 independent experiments. **b**) Perinatal nicotine-exposed pups were implanted with radio telemetry to measure arterial pressure and renal sympathetic nerve activity on Day 56 as per Fig 1a. Arterial pressure and renal sympathetic nerve activity was recorded for 7 days, and then carotid bodies were denervated and recordings recommenced for an additional 7 days. Raw traces of arterial pressure (AP) and efferent renal sympathetic nerve activity (vasoconstrictor outflow to kidneys) before carotid body denervation (Carotid body intact- BEFORE) and following carotid body denervation (Carotid body denervated- AFTER) in a representative perinatal nicotine exposed rat using telemetry. Summary statistics in n=5 perinatal nicotine rats comparing the percent change of MAP and SNA. %Change MAP (T_4=3.908), %Change SNA (T_4=3.850).

References

1. Higa R, Leonardi ML, Jawerbaum A. Intrauterine Programming of Cardiovascular Diseases in Maternal Diabetes. Front Physiol [Internet]. 2021 [cited 2024 Jan 11];12. Available from: https://www.frontiersin.org/articles/10.3389/fphys.2021.760251

2. Parada-Ricart E, Luque V, Zaragoza M, Ferre N, Closa-Monasterolo R, Koletzko B, Grote V, Gruszfeld D, Verduci E, Xhonneux A, Escribano J. Effect of maternal smoking during pregnancy on child blood pressure in a European cohort. Sci Rep. Nature Publishing Group; 2022 Oct 15;12(1):17308.

3. Palinski W. Effect of Maternal Cardiovascular Conditions and Risk Factors on Offspring Cardiovascular Disease. Circulation. American Heart Association; 2014 May 20;129(20):2066–2077.

4. Dasinger JH, Davis GK, Newsome AD, Alexander BT. Developmental Programming of Hypertension. Hypertension. American Heart Association; 2016 Oct;68(4):826–831.

5. Alexander BT, Dasinger JH, Intapad S. Fetal Programming and Cardiovascular Pathology. Compr Physiol. 2015 Apr;5(2):997–1025. PMCID: PMC4772789

6. Taylor L, Kelly B, Leeson P. Maternal Smoking and Infant Cardiovascular Physiology. Hypertension. American Heart Association; 2010 Mar;55(3):614–616.

7. Kooijman MN, Bakker H, Franco OH, Hofman A, Taal HR, Jaddoe VWV. Fetal Smoke Exposure and Kidney Outcomes in School-Aged Children. Am J Kidney Dis Off J Natl Kidney Found. 2015 Sep;66(3):412–420. PMID: 25641064

8. Nordenstam F. Prenatal nicotine exposure was associated with long-term impact on the cardiovascular system and regulation—Review. Acta Paediatr. John Wiley & Sons, Ltd; 2021 Sep 1;110(9):2536–2544.

9. Nordenstam F, Norman M, Caidahl K, Wickström R. Arterial Stiffness and Carotid Intima‐Media Thickness in Children Exposed to Smokeless Tobacco in Fetal Life. J Am Heart Assoc. Wiley; 2024 Jan 16;13(2):e9128.

10. Spindel ER, McEvoy CT. The Role of Nicotine in the Effects of Maternal Smoking during Pregnancy on Lung Development and Childhood Respiratory Disease. Implications for Dangers of E-Cigarettes. Am J Respir Crit Care Med. 2016 Mar 1;193(5):486–494. PMCID: PMC4824926

11. Oakes JM, Fuchs RM, Gardner JD, Lazartigues E, Yue X. Nicotine and the renin-angiotensin system. Am J Physiol - Regul Integr Comp Physiol. 2018 Nov 1;315(5):R895–R906. PMCID: PMC6295500

12. Ramalingam A, Budin SB, Mohd. Fauzi N, Ritchie RH, Zainalabidin S. Angiotensin II Type I Receptor Antagonism Attenuates Nicotine-Induced Cardiac Remodeling, Dysfunction, and Aggravation of Myocardial Ischemia-Reperfusion Injury in Rats. Front Pharmacol [Internet]. 2019 [cited 2024 Jan 25];10. Available from: https://www.frontiersin.org/articles/10.3389/fphar.2019.01493

13. Fried ND, Morris TM, Whitehead A, Lazartigues E, Yue X, Gardner JD. Angiotensin II type 1 receptor mediates pulmonary hypertension and right ventricular remodeling induced by inhaled nicotine. Am J Physiol Heart Circ Physiol. 2021 Apr 1;320(4):H1526–H1534. PMCID: PMC8260386

14. Mao C, Zhang H, Xiao D, Zhu L, Ding Y, Zhang Y, Wu L, Xu Z, Zhang L. Perinatal nicotine exposure alters AT1 and AT2 receptor expression pattern in the brain of fetal and offspring rats. Brain Res. 2008 Dec 3;1243:47–52. PMCID: PMC2664080

15. Xiao D, Huang X, Lawrence J, Yang S, Zhang L. Fetal and Neonatal Nicotine Exposure Differentially Regulates Vascular Contractility in Adult Male and Female Offspring. J Pharmacol Exp Ther. American Society for Pharmacology and Experimental Therapeutics; 2007 Feb 1;320(2):654–661. PMID: 17068201

16. Gao YJ, Holloway AC, Su LY, Takemori K, Lu C, Lee RMKW. Effects of fetal and neonatal exposure to nicotine on blood pressure and perivascular adipose tissue function in adult life. Eur J Pharmacol. 2008 Aug 20;590(1):264–268.

17. Paxton WG, Marrero MB, Klein JD, Delafontaine P, Berk BC, Bernstein KE. The angiotensin II AT1 receptor is tyrosine and serine phosphorylated and can serve as a substrate for the src family of tyrosine kinases. Biochem Biophys Res Commun. 1994 Apr 15;200(1):260–267. PMID: 7513159

18. Tao H, Rui C, Zheng J, Tang J, Wu L, Shi A, Chen N, He R, Wu C, Li J, Yin X, Zhang P, Zhu Z, Tao J, Xiao J, Mao C, Xu Z. Angiotensin II-mediated vascular changes in aged offspring rats exposed to perinatal nicotine. Peptides. 2013 Jun 1;44:111–119.

19. Abdala AP, McBryde FD, Marina N, Hendy EB, Engelman ZJ, Fudim M, Sobotka PA, Gourine AV, Paton JF. Hypertension is critically dependent on the carotid body input in the spontaneously hypertensive rat. J Physiol. 2012 Sep 1;590(Pt 17):4269–77.

20. McBryde FD, Abdala AP, Hendy EB, Pijacka W, Marvar P, Moraes DJ, Sobotka PA, Paton JF. The carotid body as a putative therapeutic target for the treatment of neurogenic hypertension. Nat Commun. 2013;4:2395.

21. Zera T, Moraes DJA, da Silva MP, Fisher JP, Paton JFR. The Logic of Carotid Body Connectivity to the Brain. Physiology. 2019 Jun 5;34(4):264–282. PMID: 31165684

22. Pauza AG, Thakkar P, Tasic T, Felippe I, Bishop P, Greenwood MP, Rysevaite-Kyguoliene K, Ast J, Broichhagen J, Hodson DJ, Salgado HC, Pauza DH, Japundzic-Zigon N, Paton JFR, Murphy D. GLP1R Attenuates Sympathetic Response to High Glucose via Carotid Body Inhibition. Circ Res. 2022 Mar 4;130(5):694–707. PMCID: PMC8893134

23. Stéphan-Blanchard E, Chardon K, Léké A, Delanaud S, Djeddi D, Libert JP, Bach V, Telliez F. In Utero Exposure to Smoking and Peripheral Chemoreceptor Function in Preterm Neonates. Pediatrics. American Academy of Pediatrics; 2010 Mar 1;125(3):e592–e599. PMID: 20176675

24. Argacha JF, Xhaët O, Gujic M, Adamopoulos D, Beloka S, Dreyfuss C, Degaute JP, van de Borne P. Nicotine increases chemoreflex sensitivity to hypoxia in non-smokers. J Hypertens. 2008 Feb;26(2):284–294. PMID: 18192843

25. Holgert H, Hökfelt T, Hertzberg T, Lagercrantz H. Functional and developmental studies of the peripheral arterial chemoreceptors in rat: effects of nicotine and possible relation to sudden infant death syndrome. Proc Natl Acad Sci U S A. 1995 Aug 1;92(16):7575–7579. PMCID: PMC41382

26. Prieto-Lloret J, Caceres AI, Obeso A, Rocher A, Rigual R, Agapito MT, Bustamante R, Castañeda J, Perez-Garcia MT, Lopez-Lopez JR, Gonzalez C. Ventilatory responses and carotid body function in adult rats perinatally exposed to hyperoxia. J Physiol. 2004 Jan 1;554(Pt 1):126–144. PMCID: PMC1664733

27. Nanduri J, Prabhakar NR. Epigenetic regulation of Carotid Body Oxygen Sensing: Clinical Implications. Adv Exp Med Biol. 2015;860:1–8. PMCID: PMC4870818

28. Roy A, Farnham MMJ, Derakhshan F, Pilowsky PM, Wilson RJA. Acute intermittent hypoxia with concurrent hypercapnia evokes P2X and TRPV1 receptor-dependent sensory long-term facilitation in naïve carotid bodies. J Physiol. :n/a-n/a.

29. Liu J, Yu C, Doherty TM, Akbari O, Allard P, Rehan VK. Perinatal nicotine exposure-induced transgenerational asthma: Effects of reexposure in F1 gestation. FASEB J Off Publ Fed Am Soc Exp Biol. 2020 Sep;34(9):11444–11459. PMCID: PMC7839813

30. Xiao D, Huang X, Li Y, Dasgupta C, Wang L, Zhang L. Antenatal Antioxidant Prevents Nicotine-Mediated Hypertensive Response in Rat Adult Offspring. Biol Reprod. 2015 Sep;93(3):66. PMCID: PMC4710188

31. Wongtrakool C, Wang N, Hyde DM, Roman J, Spindel ER. Prenatal Nicotine Exposure Alters Lung Function and Airway Geometry through α7 Nicotinic Receptors. Am J Respir Cell Mol Biol. 2012 May;46(5):695–702. PMCID: PMC3359906

32. Jendzjowsky NG, Roy A, Wilson RJA. Asthmatic allergen inhalation sensitises carotid bodies to lysophosphatidic acid. J Neuroinflammation. 2021 Aug 31;18:191. PMCID: PMC8408927

33. Conde SV, Sacramento JF, Guarino MP. Carotid body: a metabolic sensor implicated in insulin resistance. Physiol Genomics. 2018 01;50(3):208–214. PMID: 29373079

34. Hockman D, Adameyko I, Kaucka M, Barraud P, Otani T, Hunt A, Hartwig AC, Sock E, Waithe D, Franck MCM, Ernfors P, Ehinger S, Howard MJ, Brown N, Reese J, Baker CVH. Striking parallels between carotid body glomus cell and adrenal chromaffin cell development. Dev Biol. 2018 May 25; PMID: 29807017

35. Dixon DN, Loxley RA, Barron A, Cleary S, Phillips JK. Comparative studies of PC12 and mouse pheochromocytoma-derived rodent cell lines as models for the study of neuroendocrine systems. In Vitro Cell Dev Biol Anim. 2005 Aug;41(7):197–206. PMID: 16223334

36. Zhu WH, Conforti L, Czyzyk-Krzeska MF, Millhorn DE. Membrane depolarization in PC-12 cells during hypoxia is regulated by an O2-sensitive K+ current. Am J Physiol. 1996 Aug;271(2 Pt 1):C658-665. PMID: 8770007

37. Mariano VS, Boer PA, Gontijo JAR. Fetal Undernutrition Programming, Sympathetic Nerve Activity, and Arterial Hypertension Development. Front Physiol [Internet]. 2021 [cited 2024 Feb 6];12. Available from: https://www.frontiersin.org/journals/physiology/articles/10.3389/fphys.2021.704819

38. Eriksson J, Forsén T, Tuomilehto J, Osmond C, Barker D. Fetal and Childhood Growth and Hypertension in Adult Life. Hypertension. American Heart Association; 2000 Nov;36(5):790–794.

39. Cho NH, Silverman BL, Rizzo TA, Metzger BE. Correlations between the intrauterine metabolic environment and blood pressure in adolescent offspring of diabetic mothers. J Pediatr. 2000 May 1;136(5):587–592.

40. Walton SL, Bielefeldt-Ohmann H, Singh RR, Li J, Paravicini TM, Little MH, Moritz KM. Prenatal hypoxia leads to hypertension, renal renin-angiotensin system activation and exacerbates salt-induced pathology in a sex-specific manner. Sci Rep. Nature Publishing Group; 2017 Aug 15;7(1):8241.

41. Zhou J, Xiao D, Hu Y, Wang Z, Paradis A, Mata-Greenwood E, Zhang L. Gestational Hypoxia Induces Preeclampsia-Like Symptoms via Heightened Endothelin-1 Signaling in Pregnant Rats. Hypertension. American Heart Association; 2013 Sep;62(3):599–607.

42. Costa TJ, De Oliveira JC, Giachini FR, Lima VV, Tostes RC, Bomfim GF. Programming of Vascular Dysfunction by Maternal Stress: Immune System Implications. Front Physiol [Internet]. 2022 [cited 2024 Feb 6];13. Available from: https://www.frontiersin.org/journals/physiology/articles/10.3389/fphys.2022.787617

43. Li Y, Xiao D, Dasgupta C, Xiong F, Tong W, Yang S, Zhang L. Perinatal Nicotine Exposure Increases Vulnerability of Hypoxic-Ischemic Brain Injury in Neonatal Rats: Role of Angiotensin II Receptors. Stroke J Cereb Circ. 2012 Sep;43(9):2483–2490. PMCID: PMC3429721

44. Demura M, Demura Y, Takeda Y, Saijoh K. Dynamic regulation of the angiotensinogen gene by DNA methylation, which is influenced by various stimuli experienced in daily life. Hypertens Res. Nature Publishing Group; 2015 Aug;38(8):519–527.

45. Stéphan-Blanchard E, Bach V, Telliez F, Chardon K. Perinatal nicotine/smoking exposure and carotid chemoreceptors during development. Respir Physiol Neurobiol. 2013 Jan 1;185(1):110–119. PMID: 22743051

46. Dos Santos E, Sacramento JF, Melo BF, Conde SV. Carotid Body Dysfunction in Diet-Induced Insulin Resistance Is Associated with Alterations in Its Morphology. Adv Exp Med Biol. 2018;1071:103–108. PMID: 30357740

47. Jendzjowsky NG, Roy A, Iftinca M, Barioni NO, Kelly MM, Herrington BA, Visser F, Altier C, Wilson RJA. PKCε stimulation of TRPV1 orchestrates carotid body responses to asthmakines. J Physiol. 2021 Feb;599(4):1335–1354. PMCID: PMC7898719

48. Narkiewicz K, Ratcliffe LEK, Hart EC, Briant LJB, Chrostowska M, Wolf J, Szyndler A, Hering D, Abdala AP, Manghat N, Burchell AE, Durant C, Lobo MD, Sobotka PA, Patel NK, Leiter JC, Engelman ZJ, Nightingale AK, Paton JFR. Unilateral Carotid Body Resection in Resistant Hypertension: A Safety and Feasibility Trial. JACC Basic Transl Sci. 2016 Aug 1;1(5):313–324.

49. Niewinski P, Janczak D, Rucinski A, Tubek S, Engelman ZJ, Piesiak P, Jazwiec P, Banasiak W, Fudim M, Sobotka PA, Javaheri S, Hart ECJ, Paton JFR, Ponikowski P.

Carotid body resection for sympathetic modulation in systolic heart failure: results from first-in-man study. Eur J Heart Fail. 2017;19(3):391–400.

50. Öztürk BE, Johnson ME, Kleyman M, Turunç S, He J, Jabalameli S, Xi Z, Visel M, Dufour VL, Iwabe S, Pompeo Marinho LFL, Aguirre GD, Sahel JA, Schaffer DV, Pfenning AR, Flannery JG, Beltran WA, Stauffer WR, Byrne LC. scAAVengr, a transcriptome-based pipeline for quantitative ranking of engineered AAVs with single-cell resolution. Harvey BK, Chen L, editors. eLife. eLife Sciences Publications, Ltd; 2021 Oct 19;10:e64175.

Figure 1.

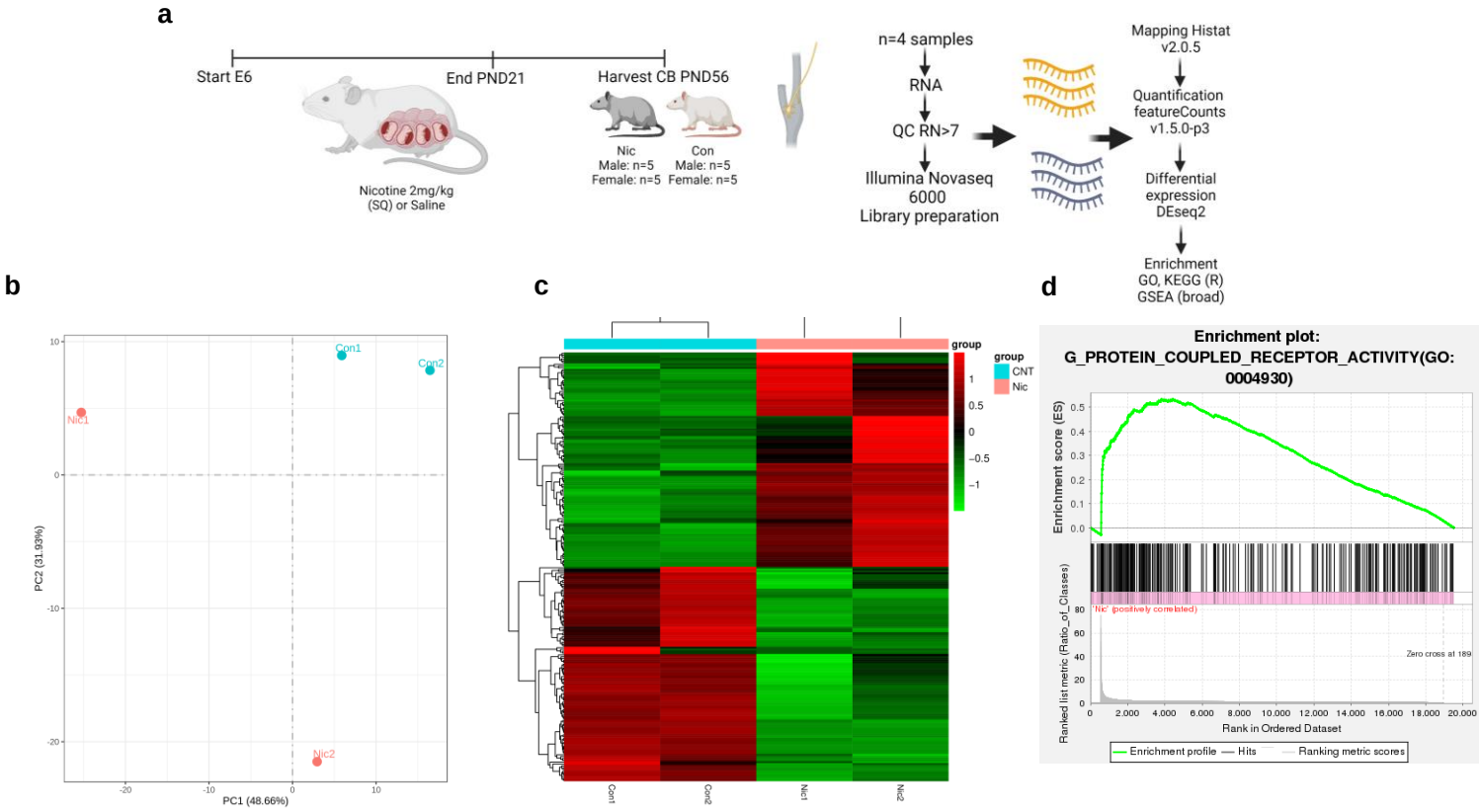
a
Start E6
End PND21
Harvest CB PND56
Nicotine 2mg/kg
(SQ) or Saline
Nic
Male: n=5
Female: n=5
Con
Male: n=5
Female: n=5
n=4 samples
RNA
QC RN>7
Illumina Novaseq
6000
Library preparation
Mapping Histat
v2.0.5
Quantification
featureCounts
v1.5.0-p3
Differential
expression
DEseq2
Enrichment
GO, KEGG (R)
GSEA (broad)
b
Con1
Con2
Nic1
Nic2
PC2 (31.93%)
PC1 (48.66%)
c
group
CNT
Nic
Con1
Con2
Nic1
Nic2
d
Enrichment plot:
G_PROTEIN_COUPLED_RECEPTOR_ACTIVITY(GO:
0004930)
Enrichment score (ES)
'Nic' (positively correlated)
Zero cross at 189
Ranked list metric (Ratio_of_Classes)
Rank in Ordered Dataset
Enrichment profile
Hits
Ranking metric scores

Figure 2.

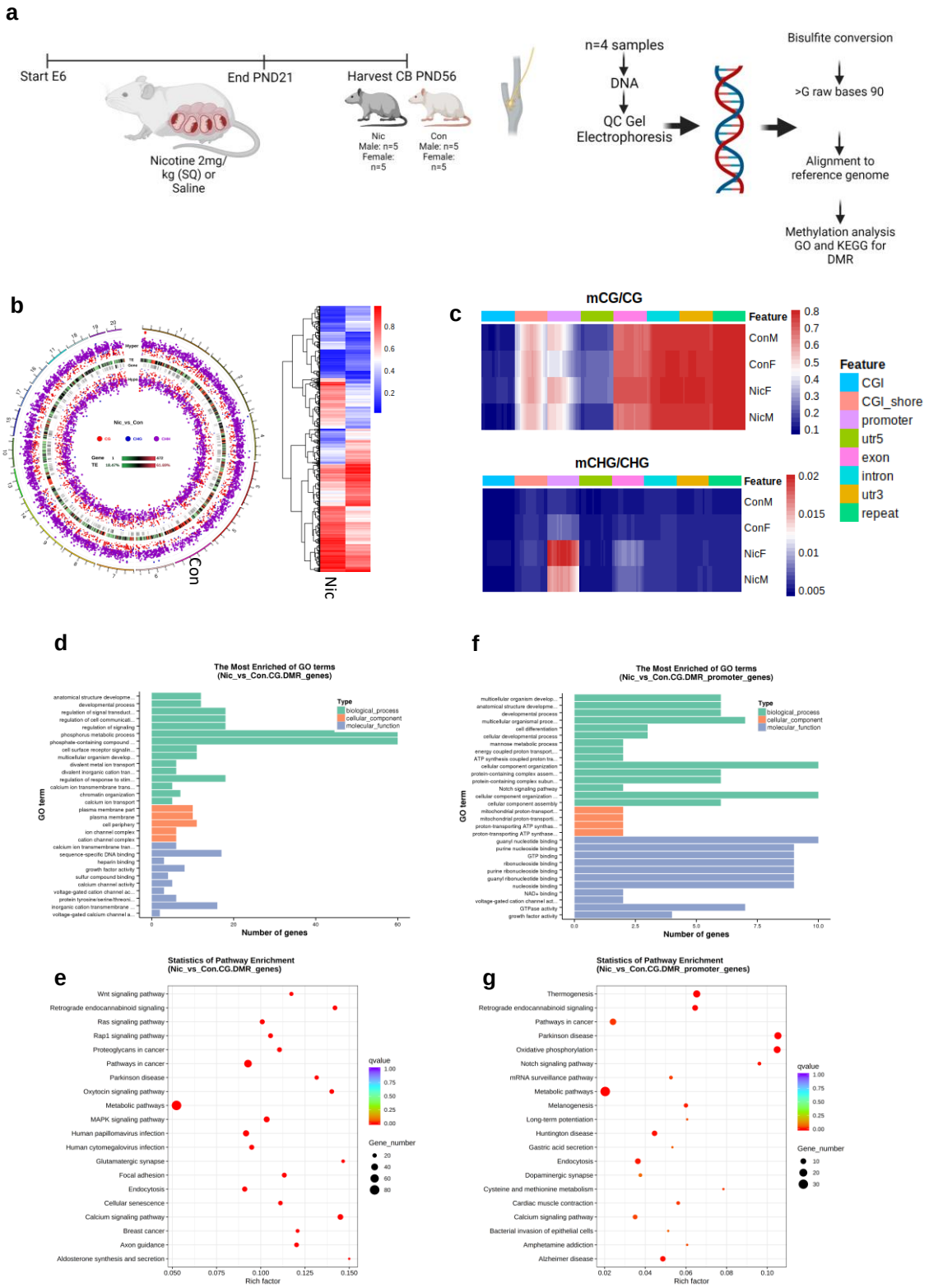
a
Start E6
End PND21
Harvest CB PND56
Nicotine 2mg/ kg (SQ) or Saline
Nic Male: n=5 Female: n=5
Con Male: n=5 Female: n=5
n=4 samples
DNA
QC Gel Electrophoresis
Bisulfite conversion
>G raw bases 90
Alignment to reference genome
Methylation analysis GO and KEGG for DMR
b
Con
Nic
c
mCG/CG
mCHG/CHG
Feature
ConM
ConF
NicF
NicM
CGI
CGI_shore
promoter
utr5
exon
intron
utr3
repeat
d
The Most Enriched of GO terms (Nic_vs_Con.CG.DMR_genes)
GO term
Number of genes
Type
biological_process
cellular_component
molecular_function
f
The Most Enriched of GO terms (Nic_vs_Con.CG.DMR_promoter_genes)
e
Statistics of Pathway Enrichment (Nic_vs_Con.CG.DMR_genes)
Wnt signaling pathway
Retrograde endocannabinoid signaling
Ras signaling pathway
Rap1 signaling pathway
Proteoglycans in cancer
Pathways in cancer
Parkinson disease
Oxytocin signaling pathway
Metabolic pathways
MAPK signaling pathway
Human papillomavirus infection
Human cytomegalovirus infection
Glutamatergic synapse
Focal adhesion
Endocytosis
Cellular senescence
Calcium signaling pathway
Breast cancer
Axon guidance
Aldosterone synthesis and secretion
Rich factor
qvalue
Gene_number
g
Statistics of Pathway Enrichment (Nic_vs_Con.CG.DMR_promoter_genes)
Thermogenesis
Retrograde endocannabinoid signaling
Pathways in cancer
Parkinson disease
Oxidative phosphorylation
Notch signaling pathway
mRNA surveillance pathway
Metabolic pathways
Melanogenesis
Long-term potentiation
Huntington disease
Gastric acid secretion
Endocytosis
Dopaminergic synapse
Cysteine and methionine metabolism
Cardiac muscle contraction
Calcium signaling pathway
Bacterial invasion of epithelial cells
Amphetamine addiction
Alzheimer disease
Rich factor
qvalue
Gene_number

Figure 3.

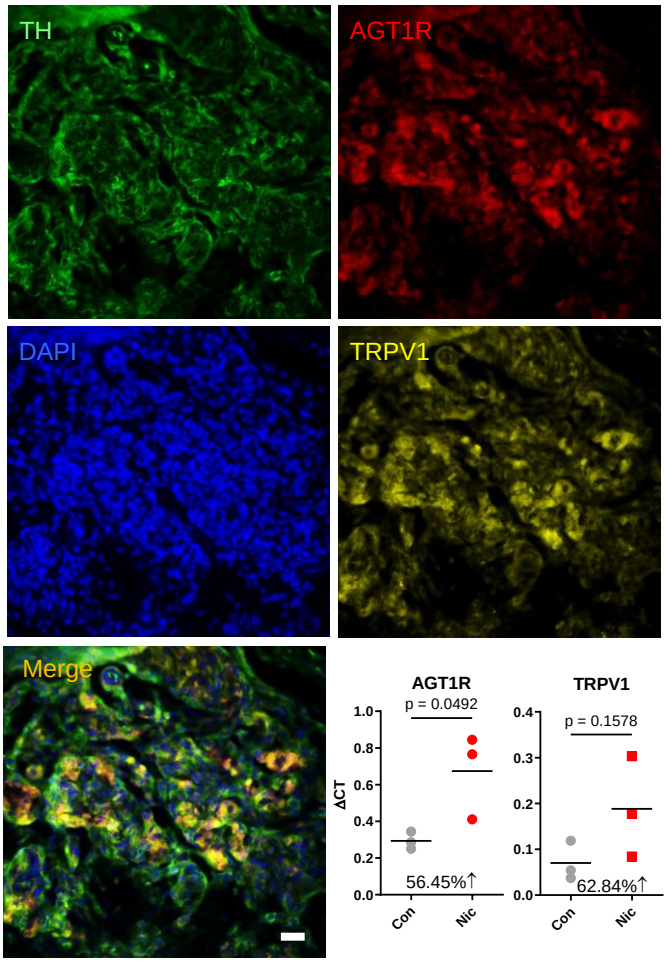
TH
AGT1R
DAPI
TRPV1
Merge
AGT1R
p = 0.0492
ΔCT
1.0
0.8
0.6
0.4
0.2
0.0
56.45%↑
Con
Nic
TRPV1
p = 0.1578
0.4
0.3
0.2
0.1
0.0
62.84%↑
Con
Nic

Figure 4.

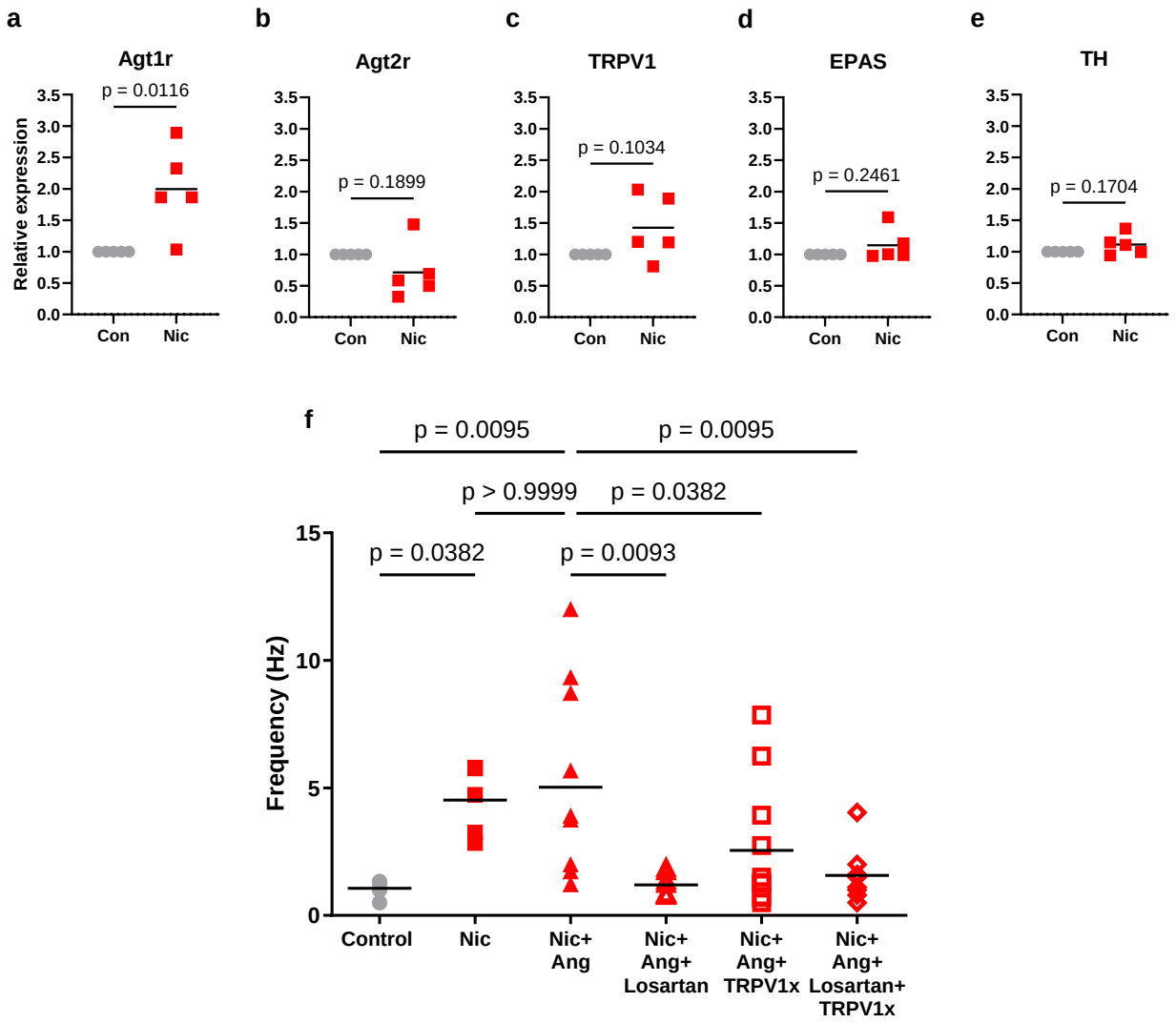
a
Agt1r
p = 0.0116
Relative expression
3.5
3.0
2.5
2.0
1.5
1.0
0.5
0.0
Con
Nic
b
Agt2r
p = 0.1899
c
TRPV1
p = 0.1034
d
EPAS
p = 0.2461
e
TH
p = 0.1704
f
p = 0.0095
p = 0.0095
p > 0.9999
p = 0.0382
p = 0.0382
p = 0.0093
Frequency (Hz)
15
10
5
0
Control
Nic
Nic+ Ang
Nic+ Ang+ Losartan
Nic+ Ang+ TRPV1x
Nic+ Ang+ Losartan+ TRPV1x

Figure 5.

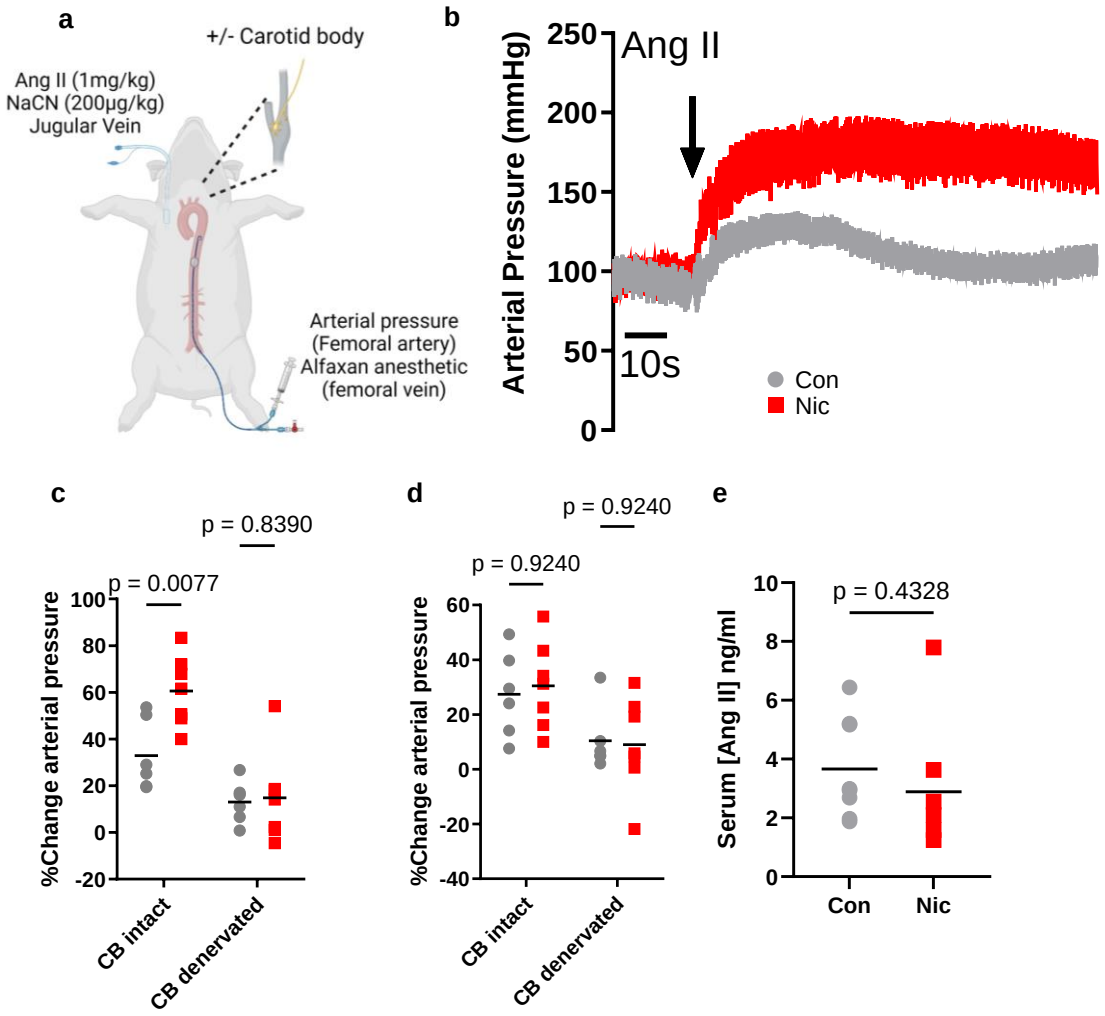
a
+/- Carotid body
Ang II (1mg/kg)
NaCN (200µg/kg)
Jugular Vein
Arterial pressure
(Femoral artery)
Alfaxan anesthetic
(femoral vein)
b
Ang II
Arterial Pressure (mmHg)
250
200
150
100
50
0
10s
Con
Nic
c
p = 0.8390
p = 0.0077
%Change arterial pressure
100
80
60
40
20
0
-20
CB intact
CB denervated
d
p = 0.9240
p = 0.9240
%Change arterial pressure
60
40
20
0
-20
-40
CB intact
CB denervated
e
p = 0.4328
Serum [Ang II] ng/ml
10
8
6
4
2
0
Con
Nic

Figure 6.

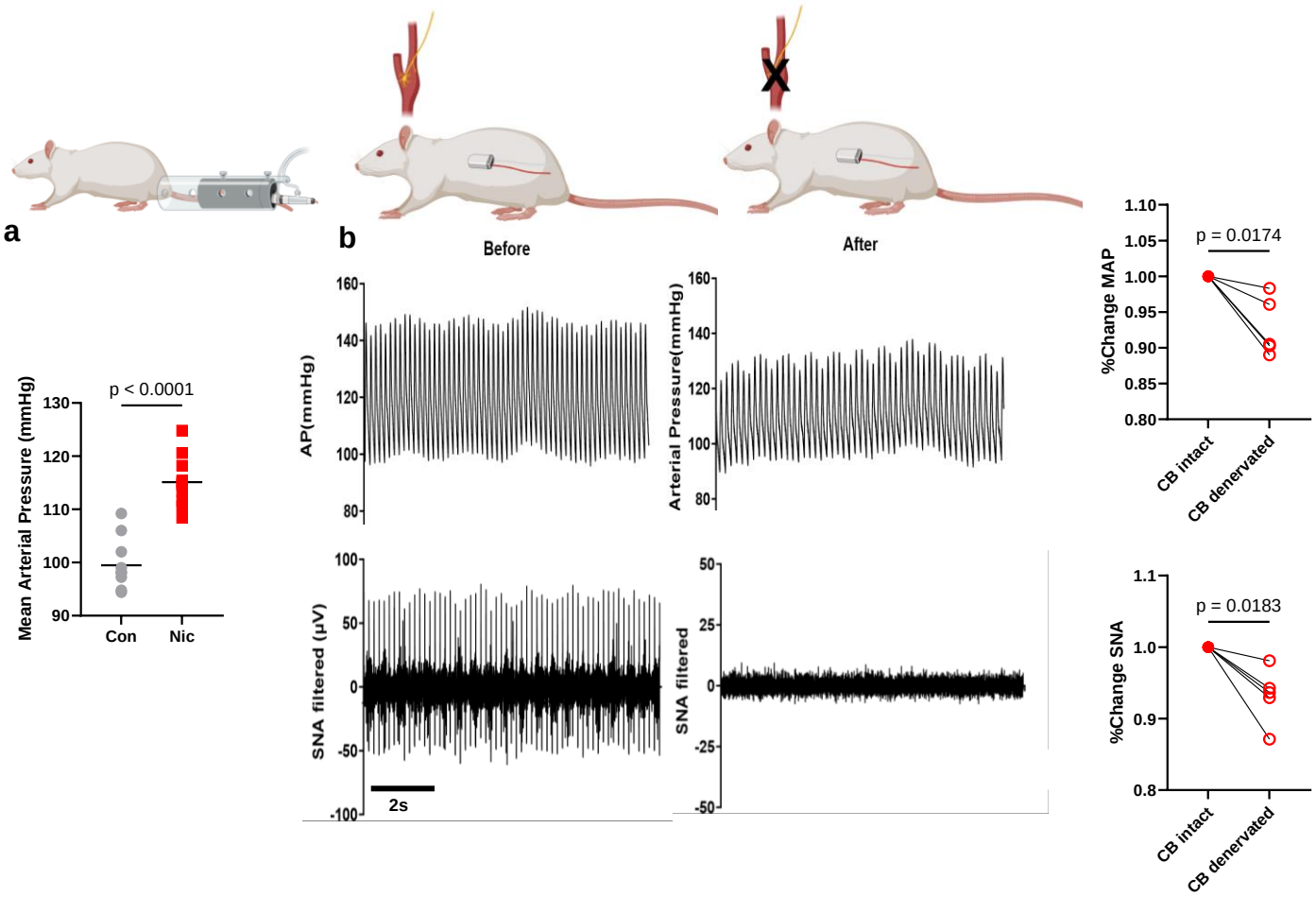
a
b
Before
After
Mean Arterial Pressure (mmHg)
p < 0.0001
Con
Nic
AP(mmHg)
Arterial Pressure(mmHg)
SNA filtered (μV)
SNA filtered
2s
%Change MAP
p = 0.0174
CB intact
CB denervated
%Change SNA
p = 0.0183
CB intact
CB denervated